

Supplementary materials

Self-assembled Photonic structure: Ga optical antenna on GaP Nanowire

Alexey Kuznetsov^{a,b}, Prithu Roy^{c,d}, Dmitry V. Grudinin^e, Valeriy M. Kondratev^b, Svetlana A. Kadinskaya^b, Alexandr A. Vorobyev^b, Konstantin P. Kotlyar^b, Evgeniy V. Ubyivovk^a, Vladimir V. Fedorov^b, George E. Cirlin^a, Ivan S. Mukhin^{b,d,f}, Aleksey V. Arsenin^e, Valentyn S. Volkov^e, Alexey D. Bolshakov^{a,b,e*}

^a St. Petersburg State University, St. Petersburg 199034, Russia;

^b Center for nanotechnologies, Alferov University, Saint Petersburg 194021, Russia;

^c Aix Marseille Univ, CNRS, Centrale Marseille, Institut Fresnel, AMUTech, Marseille 13013, France (current affiliation);

^d ITMO University, 197101, Saint Petersburg, Russia;

^e Center for Photonics and 2D Materials, Moscow Institute of Physics and Technology, Dolgoprudny 141701, Russia

^f Higher School of Engineering Physics, Peter the Great Saint Petersburg Polytechnic University, Saint Petersburg 195251, Russia

*corresponding author bolshakov@live.com

Elemental mapping of the NWs

To study the composition of the grown NWs we carried out additional measurements using high resolution transmission electron microscopy (TEM, Zeiss Libra 200 FE) equipped with energy-dispersive X-ray spectroscopy (EDX). We collected 8 EDX line scans studying both of the Samples and considering spatial distribution of Ga, P and As atoms along the NW axis. The first scan presented in Fig. S1a collected from individual pristine GaP NW of the Sample 1 demonstrates a clear stoichiometric ratio of 1 between Ga and P species without any noticeable doping.

Fig. S1b demonstrates elemental mapping along the topmost (7th) GaPAs insert of individual NW of the Sample 2. Here, presence of As is clearly demonstrated with the highest content of about 22 atomic percent (44 molar percent of GaAs in GaPAs ternary alloy). Rise of the As content leads to the anticipated fall of P content without breaking of the stoichiometric $(P+As)/Ga = 1$ ratio corresponding to the crystallinity of the NW. The distributions of As and P were fitted

with the Gaussians to demonstrate their normal spatial distribution along the NW axis. The effective thickness of the insert as FWHM of the Gaussian fit is found at 50 nm, corresponding well to the growth protocol and results of analysis of the SEM images. We assume that such a documented Gaussian distribution is the result of slight inclination of the sample during the measurement providing non-orthogonal incidence of the electron beam. Importantly, the As content is found negligible below and above 60nm from the insert centerline. This is the manifestation of absence of unintentional doping of the pristine GaP segments during the growth of GaPAs inserts.

The As content was measured for all of the GaPAs inserts along one individual NW, the corresponding EDX scans are shown in Fig. S1c. The obtained data demonstrate increase of As content towards the NW top with the first (the bottom most) insert having $\text{GaP}_{0.65}\text{As}_{0.35}$ composition and the sixth - $\text{GaP}_{0.5}\text{As}_{0.5}$. This phenomenon can be governed by decrease of the substrate surface influence in terms of P diffusion with elongation of a NW. Nevertheless, all of the insertions demonstrate similar Gaussian spatial distribution of As fraction.

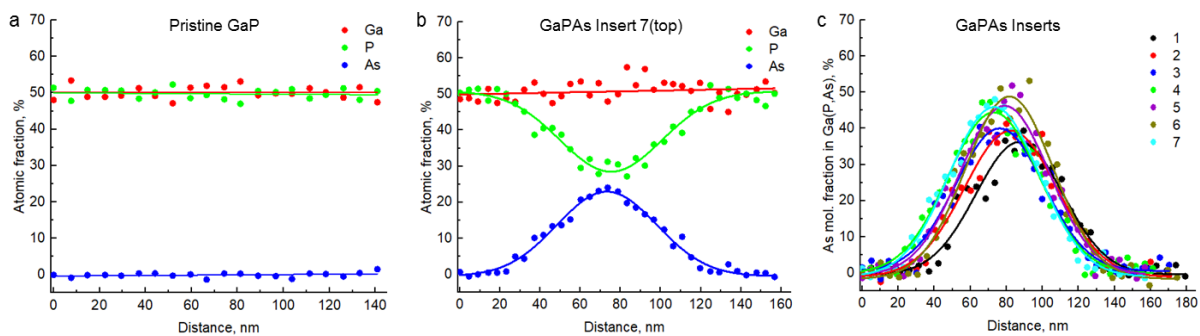


Fig. S1 | Elemental mapping of individual NWs. EDX line scans: a) Sample 1 pristine GaP NW; b) top 7th GaPAs insert of heterostructured Sample 2 GaPAs NW; c) As fraction of all the inserts of the same heterostructured NW.

Raman details

In order to exclude possible effects associated with the heating of the NW or its chemical/structural degradation during the measurements, we mapped several NWs multiple times starting from the opposite edges with Ga droplet and without it. Typical integral intensity maps of the single NW that were obtained starting from both edges are demonstrated in Fig. S2. Between the measurements (Fig. S2 (a) and (b)) the substrate was rotated 180°. As can see, the spectra measured in

the marked points (Fig. S2 (c) and (d)) exhibit similar amplitude thus the scan starting point does not affect the results.

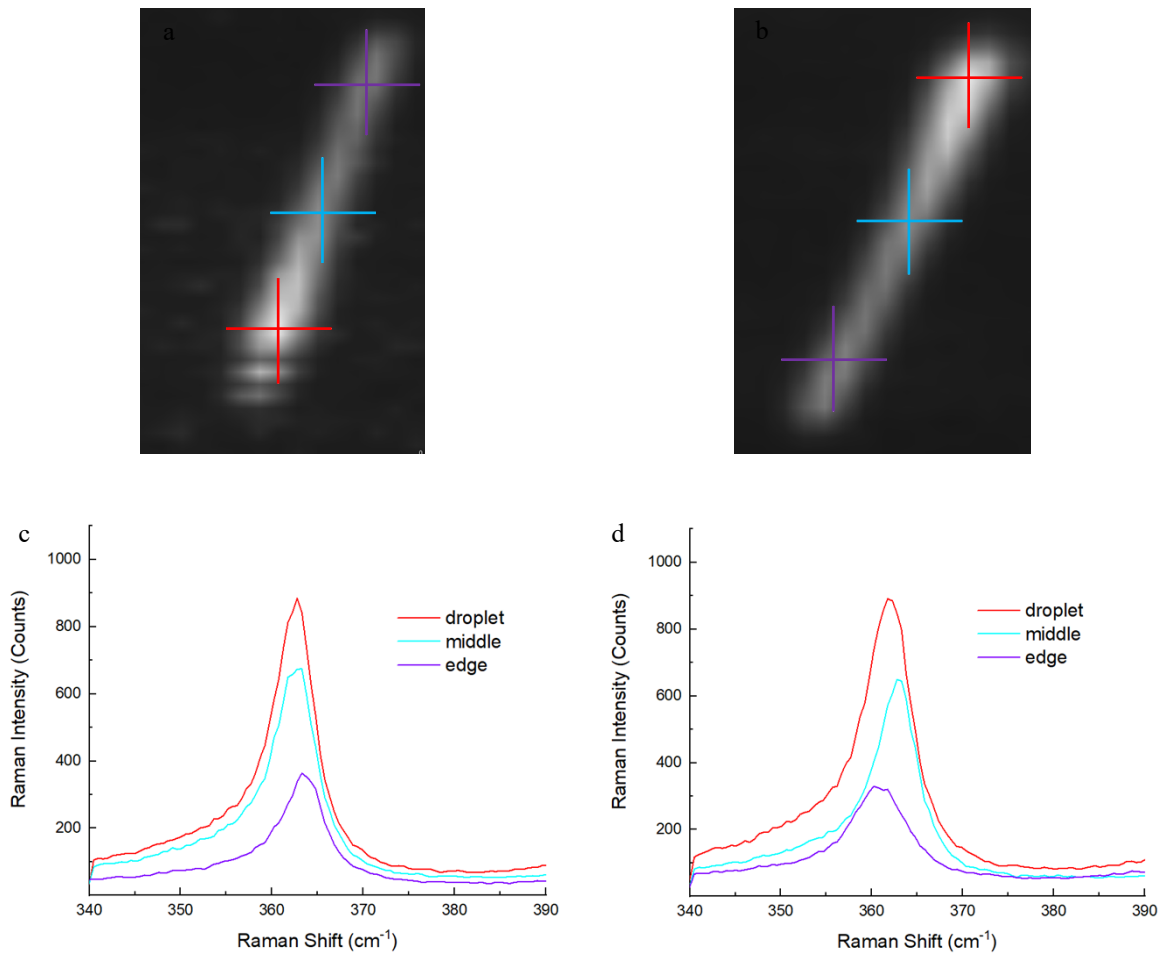


Fig. S2 | Raman integral intensity maps: (a) scanning was started from the droplet side and (b) from the edge without droplet, (c-d) corresponding Raman spectra measured in red, cyan and violet points

Spectrometer sensitivity details

To avoid the effects of the spectrometer sensitivity to the polarization orientation we measured reference spectra on Si (111) substrate (Fig. S3) in orthogonal polarizations. It's evident that both spectra are equal and demonstrate the same intensity as it was expected.

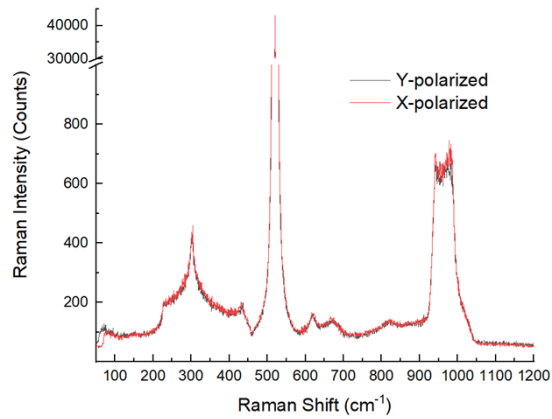


Fig. S3 | Raman spectra of Si substrate measured in vertical (Y) and horizontal (X) orientations of the polarization plane.

Numerical simulation of the PL spectra

To numerically quantify the PL spectrum of the heterostructured GaPAs NW we carried out a simulation with Ansys Lumerical. The heterostructured NW was modeled as a hexagonal prism with a diameter of 160 nm and length of 7.4 μm according to the SEM data for the experimentally studied NW. $\text{GaP}_x\text{As}_{1-x}$ inserts were not taken into consideration because of the very low contrast between GaP and $\text{GaP}_x\text{As}_{1-x}$ refractive indices. On the top edge of the NW Ga droplet was represented as a hemisphere with a radius of 80 nm. The NW was planarized on SiO_2 substrate with 50 nm ITO layer according to the experiment geometry (Fig. S4).

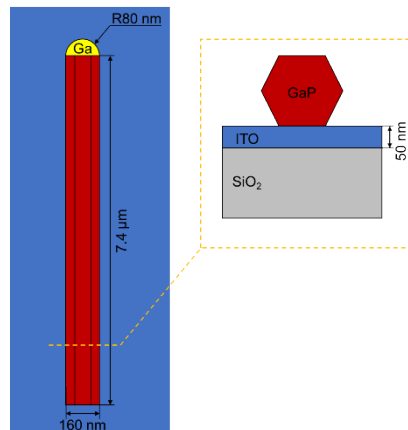


Fig. S4 | Schematics of the NW in the numerical model of the PL emission.

Multiple dipole sources with Gaussian spectrum (centered according to the peak intensity of the documented PL in Fig. 3e, Main text) were located near the NW edge without the Ga droplet to simulate the excited PL signal. In the time domain the pulse duration was 17 fs. The PL spectrum was calculated by integrating (Fourier transform) the electric field ($E(t)$) in the time domain after the first 200 fs till the end of the simulation to avoid the influence of the source pulses on the calculation. The normalized calculated spectrum and experimental spectrum collected in the vicinity of the droplet edge

are shown in the Fig. 3f, Main text. The obtained spectra demonstrate excellent agreement with spectral coincidence of the F-P modes. Insufficient amplitude discrepancies occur due to the imperfections of the real NW geometry such as uneven cleave of the bottom facet, effects provided by the slight optical contrast of the $\text{GaP}_x\text{As}_{1-x}$ inserts and PL spectrum of the inserts having non-Gaussian shape, in contrast to the dipole spectrum.

For evaluation of the Purcell factor (F_p) of a NW acting as a cavity, analytical approach with the use of experimental and numerical data is used. The F_p value is evaluated along the conventional expression:

$$F_p = \frac{3}{4\pi^2} \left(\frac{\lambda}{n}\right)^3 \frac{Q}{V} \quad (1),$$

where λ - wavelength in vacuum, n - cavity refractive index, Q - quality factor of the cavity, V - mode volume.

To estimate the Q value, the peaks corresponding to the F-P modes in the PL spectrum (Fig. 3e, Main text) were fitted with Lorentz function. The F-P mode with the highest Q -factor value (~180) corresponds to the mode wavelength of 687 nm. For this mode, the refractive index of GaP is 3.2636¹.

Mode volume could not be evaluated from the obtained experimental data. As such, numerical simulation was utilized. Resonant mode was simulated with the previously used model and mode source placed at the NW end facet without the Ga droplet. Further, mode volume was calculated according the expression:

$$V = \frac{\int_V \varepsilon(r) |E(r)|^2 d^3r}{\max_{r \in V} (\varepsilon(r) |E(r)|^2)}$$

(2),

where $\varepsilon(r)$ - dielectric permittivity, $E(r)$ - electric field. The calculated mode volume is found at 0.047 μm^3 and the corresponding F_p factor is 2.73.

The value of the Purcell factor is mainly limited with Q value, which is governed by the reported efficient internal reflection by the Ga droplet and limited with a poor reflectivity of the opposite end facet. Further increase of the Purcell factor can be obtained via formation of Bragg reflector in the bottom part of the NW which is possible with the MBE technique and is assumed promising for nanoscale lasing applications. This will be the goal for our future projects.

References

1 Aspnes, D. E., & Studna, A. A. (1983). Dielectric functions and optical parameters of si, ge, gap, gaas, gasb, inp, inas, and insb from 1.5 to 6.0 ev. *Physical review B*, **27**(2), 985.